Global Change Biology
celebrating 20 years
Global Change Biology (2014), doi: 10.1111/gcb.12760

Climatic variability, hydrologic anomaly, and methane emission can turn productive freshwater marshes into net carbon sources

HOUSEN CHU[1], JOHAN F. GOTTGENS[1], JIQUAN CHEN[1], GE SUN[2], ANKUR R. DESAI[3], ZUTAO OUYANG[1], CHANGLIANG SHAO[1,4] and KEVIN CZAJKOWSKI[5]

[1]*Department of Environmental Sciences, University of Toledo, Toledo, OH, USA,* [2]*Eastern Forest Environmental Threat Assessment Center, USDA Forest Service, Raleigh, NC, USA,* [3]*Department of Atmospheric and Oceanic Sciences, University of Wisconsin-Madison, Madison, WI, USA,* [4]*Lake Erie Center, University of Toledo, Oregon, OH, USA,* [5]*Department of Geography and Planning, University of Toledo, Toledo, OH, USA*

Abstract

Freshwater marshes are well-known for their ecological functions in carbon sequestration, but complete carbon budgets that include both methane (CH_4) and lateral carbon fluxes for these ecosystems are rarely available. To the best of our knowledge, this is the first full carbon balance for a freshwater marsh where vertical gaseous [carbon dioxide (CO_2) and CH_4] and lateral hydrologic fluxes (dissolved and particulate organic carbon) have been simultaneously measured for multiple years (2011–2013). Carbon accumulation in the sediments suggested that the marsh was a long-term carbon sink and accumulated ~96.9 ± 10.3 (±95% CI) g C m^{-2} yr^{-1} during the last ~50 years. However, abnormal climate conditions in the last 3 years turned the marsh to a source of carbon (42.7 ± 23.4 g C m^{-2} yr^{-1}). Gross ecosystem production and ecosystem respiration were the two largest fluxes in the annual carbon budget. Yet, these two fluxes compensated each other to a large extent and led to the marsh being a CO_2 sink in 2011 (−78.8 ± 33.6 g C m^{-2} yr^{-1}), near CO_2-neutral in 2012 (29.7 ± 37.2 g C m^{-2} yr^{-1}), and a CO_2 source in 2013 (92.9 ± 28.0 g C m^{-2} yr^{-1}). The CH_4 emission was consistently high with a three-year average of 50.8 ± 1.0 g C m^{-2} yr^{-1}. Considerable hydrologic carbon flowed laterally both into and out of the marsh (108.3 ± 5.4 and 86.2 ± 10.5 g C m^{-2} yr^{-1}, respectively). In total, hydrologic carbon fluxes contributed ~23 ± 13 g C m^{-2} yr^{-1} to the three-year carbon budget. Our findings highlight the importance of lateral hydrologic inflows/outflows in wetland carbon budgets, especially in those characterized by a flow-through hydrologic regime. In addition, different carbon fluxes responded unequally to climate variability/anomalies and, thus, the total carbon budgets may vary drastically among years.

Keywords: carbon budget, carbon dioxide, carbon sequestration, dissolved organic carbon, eddy-covariance, methane, particulate organic carbon

Received 24 April 2014 and accepted 10 September 2014

Introduction

Global carbon and water cycles are highly coupled at multiple scales. Studies show that lateral hydrologic carbon fluxes (i.e., carbon transported via runoff) are important vectors in regional carbon cycling (Algesten *et al*., 2004; Cole *et al*., 2007). Carbon sequestered by terrestrial ecosystems (e.g., forests, croplands) may be leached out, carried along aquatic pathways, and buried in low areas of landscapes (e.g., wetlands, lakes) (Mccarty & Ritchie, 2002; Bedard-Haughn *et al*., 2006; Bridgham *et al*., 2006; Buffam *et al*., 2011). Thus, these hydrologic processes are significant in transporting and redistributing carbon along the terrestrial-aquatic continuum (Jenerette & Lal, 2005; Cole *et al*., 2007; Johnson *et al*., 2008; Aufdenkampe *et al*., 2011).

There is also growing evidence showing that inland aquatic ecosystems (e.g., rivers, wetlands, lakes) are more than just 'neutral pipes' that merely convey terrestrial carbon to the ocean (Cole *et al*., 2007; Tranvik *et al*., 2009; Aufdenkampe *et al*., 2011). The imported carbon may be transformed within the aquatic ecosystems, released via carbon dioxide (CO_2)/methane (CH_4) outgassing, or deposited in the sediment (Kling *et al*., 1991; Algesten *et al*., 2004; Cole *et al*., 2007; Tranvik *et al*., 2009; Einola *et al*., 2011). Previous studies (mostly in lakes) showed that outgassing and sedimentation processes occur simultaneously (i.e., a bidirectional carbon process) (Cole *et al*., 2007; Tranvik *et al*., 2009; Buffam *et al*., 2011; Knoll *et al*., 2013). These bidirectional characteristics draw attention to the

Correspondence: Housen Chu, tel. 419 530 2664, fax 419 530 4421, e-mail: hchu6@rockets.utoledo.edu

importance of lateral carbon transports (i.e., allochthonous carbon). Bridgham *et al*. (2006) identified freshwater mineral-soil wetlands (e.g., marshes) as the largest unknown in the North American wetland carbon budget. As these wetlands are characterized with a flow-through hydrologic regime, the interplay of autochthonous and allochthonous carbon become crucial and caution is required in interpreting the carbon sequestration rates (Bridgham *et al*., 2006).

Our previous study found that a Lake Erie coastal marsh in northwestern Ohio, United States had two-year average net ecosystem CH_4 exchanges (F_{CH4}) up to ~50 g C m^{-2} yr^{-1} (Chu *et al*., 2014b). The carbon released via F_{CH4} was compatible with the carbon uptake by net ecosystem CO_2 exchange (F_{CO2}) at the marsh (two-year average: −20.1 g C m^{-2} yr^{-1}) and led to a slight source for the atmospheric carbon budget. Gottgens & Liptak (1998) and Spongberg *et al*. (2004) showed that this marsh, on a long-term basis, served as a carbon sink according to the carbon accumulation trend in the sediment (59–69 g C m^{-2} yr^{-1}; 1920–1997 average). These findings imply a bidirectional carbon process and allochthonous carbon may supplement the marsh carbon balance. Yet, prior studies were conducted at different time spans and lacked details on lateral hydrologic carbon flows. Thus, a comprehensive picture of the marsh carbon budget was not clear.

We conducted three-year intensive and comprehensive field measurements on the F_{CO2}, F_{CH4}, and lateral hydrologic carbon flux at a Lake Erie coastal marsh. In addition, the long-term sedimentation rate of the marsh was updated. We aimed at addressing the following questions: (i) Is the three-year carbon budget (i.e., F_{CO2}, F_{CH4}, and lateral hydrologic carbon fluxes) compatible with the long-term carbon sedimentation rate at the marsh? (ii) What are the relative contributions of F_{CO2}, F_{CH4}, and lateral hydrologic carbon fluxes in the annual marsh carbon budget? (iii) What is the seasonal and interannual variability in the hydrologic carbon fluxes? (iv) To what extent do these carbon fluxes and their budgets respond to interannual climate variability? While short-term (half-hourly to seasonal) F_{CO2} and F_{CH4} dynamics and their controlling factors have been thoroughly examined in our earlier study (Chu *et al*., 2014b), the focus here is on the interannual variability and total ecosystem carbon budget.

Method

Site information

The marsh is located in the Winous Point Marsh Conservancy along the shore of Lake Erie (N41°27′51.28″, W82°59′45.02″). The 129 ha marsh is covered with a mix of emergent (*Typha angustifolia* L., *Sparganium americanum* N., *Hibiscus moscheutos* L.) and floating-leaved vegetation (*Nymphaea odorata* A., *Nelumbo lutea* W.) interspersed with areas of open water with some submerged plants (Figure S1). The dominant vegetation is *Typha* (narrow-leaved cattail) and *Nymphaea* (water lily) in the emergent and floating-leaved vegetation areas, respectively. *Nymphaea* usually starts growing petioles and leaves around late May that gradually cover the floating-leaved vegetation area from June to September. *Nymphaea* leaves start to senesce around late September and the area gradually turns to open water through the winter. On the other hand, *Typha* starts tillering and emerging around mid-May and senesces around early October. After that, much of the aboveground litter remains standing and gradually fragmentizes and deposits into the sediment through the winter and spring. Above- and belowground biomass (±SD) in the peak growing season is 0.22 ± 0.03 and 0.21 ± 0.10 kg C m^{-2} in the floating-leaved area and 1.52 ± 0.27 and 12.55 ± 3.87 kg C m^{-2} in the emergent vegetation area (Chu *et al*., 2014b). The soil organic layer extends to a depth of ~20 cm and the organic carbon storage (±SD) is around 5.32 ± 0.13 kg C m^{-2}. The surface water at the marsh has pH values of 7.18–8.63. The ice/snow cover periods are from early December to late February.

The hydrology of the marsh is relatively isolated by the surrounding dikes but agricultural runoff enters through three free-flowing culverts, with diameters of 1.8, 0.9, and 1.5 m, connecting to adjacent ditches (Gottgens & Liptak, 1998) (Figure S1). The upstream area of these ditches is dominated by conventional croplands (soybean, corn, and wheat), most of which is drained by subsurface tiles that empty into ditches. The actual watershed area was difficult to delineate in this flat landscape and different areas (200–900 ha) were reported in previous studies (Gottgens & Liptak, 1998; Muller, 2004; Spongberg *et al*., 2004). In this study, we adopted a relatively conservative estimate of ~260 ha (Figure S1). The outflow of the marsh is connected downstream to Sandusky Bay (into Lake Erie) through a manually controlled outflow gate. The gate is managed by the Winous Point Shooting Club to maintain year-round inundation at the marsh, with surface water levels ranging in depths of 0.3–0.9 m (Gottgens & Liptak, 1998; Chu *et al*., 2014b).

Micrometeorological measurements

A 3-m tower was constructed in 2010 at the center of the marsh with at least a 250-m fetch in all directions (Figure S1). Micrometeorological variables were measured at the tower including long-/short-wave radiation, photosynthetically active radiation (PAR), air temperature (T_a), and precipitation (PP) (Table S1). Two levels of sediment temperature (T_g; two replicates at 0.1 and 0.3 m depth) and surface water temperature (T_w; two replicates, 0.1 and 0.3 m above the sediment surface) were measured near the tower and the averages were used for following analyses (Table S1). The surface water table (WT) was measured during the ice-free season (Table S1). All of the variables were recorded every 30 min by a datalogger [CR5000, Campbell Sci., Inc. (CSI), Logan, UT, USA]. Regional long-

term air temperatures and precipitation were obtained through the National Climatic Data Center of the National Oceanic and Atmospheric Administration, USA.

Net ecosystem CO_2 and CH_4 exchanges

The eddy-covariance method was applied to quantify the half-hourly F_{CO2}, F_{CH4}, and evapotranspiration (ET) (Chu *et al.*, 2014b). The system comprises of a sonic anemometer (CSAT3, CSI), an open-path CO_2/H_2O infrared gas analyzer (LI7500, LI-COR, Inc. (LI-COR), Lincoln, NE, USA), and an open-path CH_4 gas analyzer (LI7700, LI-COR). The measurement periods were January, 2011 to December, 2013 for F_{CO2} and ET and March, 2011 to December, 2013 for F_{CH4}.

The half-hourly F_{CO2}, F_{CH4}, and ET were calculated and quality controlled by using the EdiRe (University of Edinburgh, v1.5.0.29, 2011) following the workflow in Chu *et al.* (2014a,b). We ran footprint analyses for each half hour (Kormann & Meixner, 2001) and the majority (>80%) of our measured fluxes originated from the 0–250 m fetch near the tower (Figure S1), within which floating-leaved vegetation area contributed ~71% to the measured fluxes (Chu *et al.*, 2014b). In this study, positive F_{CO2}, F_{CH4}, and ET indicated a net flux from the ecosystem to the atmosphere. Overall, 63% of F_{CO2} and ET passed the quality controls (Table S2) and the data gaps were filled by using the marginal distribution sampling (MDS) method (Reichstein *et al.*, 2005). F_{CO2} was further partitioned into gross ecosystem production (GEP) and ecosystem respiration (ER) following Reichstein *et al.* (2005) (Data S1.1). We adopted an eight-day non-overlapping window in fitting the ER and GEP models. The Lloyd and Taylor respiration model and the rectangular hyperbola model were adopted, respectively, in ER and GEP modeling (Lloyd & Taylor, 1994; Falge *et al.*, 2001):

$$\mathrm{ER} = R_{\mathrm{ref}} \exp\left[E_0\left(\frac{1}{T_{ref} - T_0} - \frac{1}{T_a - T_0}\right)\right] \quad (1)$$

$$\mathrm{GEP} = -\frac{\alpha P_{\max} \mathrm{PAR}}{\alpha \mathrm{PAR} + P_{\max}} \quad (2)$$

where R_{ref} (μmol CO_2 m^{-2} s^{-1}) is the base respiration at the reference temperature (T_{ref}, set as 10 °C), E_0 (°C) is the temperature sensitivity, and T_0 is set as −46.02 °C. α is the ecosystem light use efficiency (μmol CO_2 mmol quanta^{-1}), and $P_{\max}$ is the maximum CO_2 uptake rate at light saturation (μmol CO_2 m^{-2} s^{-1}). We adopted respectively negative and positive sign conventions for GEP and ER (F_{CO2} = GEP + ER). The growing and nongrowing seasons were separated by the first and last consecutive 3 days with daily absolute GEPs larger than 1 g C m^{-2} day^{-1}.

Overall, 42% of F_{CH4} passed the quality checks (Table S2). The data gaps were filled by the subsequent steps (Data S1.2): (i) Those days with short gaps in half-hourly F_{CH4} (<1.5 hour consecutively and <12 hour in total daily) were filled using the MDS method (Reichstein *et al.*, 2005); (ii) Those days with longer gaps were filled using the empirical regression models at the daily scale with a predictor variable of T_g (Chu *et al.*, 2014b):

$$\ln(F_{\mathrm{CH_4}} \times 10^3) = \ln(R_{\mathrm{FCH_4}} \times 10^3) + S_{Tg}(T_g - \bar{T}_g) \quad (3)$$

where the overbar indicates the mean value of the study period, R_{FCH4} (g C m^{-2} day^{-1}) is the base daily F_{CH4} (g C m^{-2} day^{-1}) at the averaged T_g (14 °C), and S_{Tg} represents the sensitivity of F_{CH4} to change in the daily T_g.

We assessed the uncertainties of F_{CO2}, F_{CH4}, and ET via calculating the random errors (Richardson *et al.*, 2006) and the uncertainties originated from friction velocity criteria selection, gap-filling and flux-partitioning procedures (Aurela *et al.*, 2002; Reichstein *et al.*, 2005; Richardson & Hollinger, 2005; Desai *et al.*, 2008) (Data S1.3). In addition, the energy balance closure was examined for both the annual and daily integrals of energy fluxes/storage changes (Mahrt, 1998; Wilson *et al.*, 2002) (Data S1.4). The annual energy balance ratio averaged 0.72 (0.64–0.76 for each year) over the 3 years (Table S3). Our energy balance closure was slightly lower than the reported cross-site average (~0.80, Wilson *et al.*, 2002) but was still within the reported range from a few available studies at wetlands [0.76 ± 0.13 (±SD), Stoy *et al.*, 2013] and small lakes (0.72–0.82, Nordbo *et al.*, 2011).

Lateral hydrologic carbon fluxes

Lateral hydrologic carbon fluxes were calculated from the water discharges (inflow and outflow) and water carbon concentrations in the ice-free periods (26 February to 8 December in 2011, 13 February to 21 December in 2012, and 23 February to 5 December in 2013). The water inflows and outflows were obtained by solving the marsh water budget at a daily scale:

$$Q_{\mathrm{net}} = \mathrm{PP} - \mathrm{ET} - \Delta\mathrm{WT} \quad (4)$$

where ΔWT and PP are the measured daily surface water level change (mm day^{-1}) and precipitation (mm day^{-1}) at the tower. ET is obtained by the eddy-covariance method (mm day^{-1}). Q_{net} (mm day^{-1}) is the net lateral water flow normalized for marsh area. Groundwater flow was assumed negligible in Q_{net}, because the area is dominated by clay-rich soil/sediment characterized by low permeability and percolation rates (Muller, 2004). The upstream croplands are drained using tiles and this drainage flows mostly into ditches before entering the marsh. We adopted the sign convention that PP has positive or zero values. Positive Q_{net} indicates a net flux out of the marsh and positive ΔWT indicated net increases of WT. We further partitioned the Q_{net} into the water flows at the three inlets (Q_{in}; mm day^{-1}) and one outlet (Q_{out}; mm day^{-1}) by identifying the periods with the outflow gate opened/closed (Data S2.1–S2.3).

Hydrologic carbon concentration

The water carbon concentrations were sampled manually during the ice-free periods and the sampling intervals were ~16, ~21, and ~19 days in 2011, 2012, and 2013, respectively. Two 500 ml bottles (Nalgene) of water were taken at each of the three inlets and near the tower during a total of 42 sampling trips. The outlet water samples were only taken during

the periods when the outflow gate was opened (17 trips). For each trip/location, three 100 ml subsamples were taken in lab from the well-mixed 1000 ml water sample. Particulate organic carbon (POC) and dissolved organic carbon (DOC) were separated via preashed and preweighted Millipore (0.45 μm pore size, APFF) filters. Organic carbon content was estimated by using the weight loss on ignition method (Dean, 1974; Heiri *et al*., 2001) (Data S2.4). Starting in March, 2013, additional measures were taken to determine the dissolved inorganic carbon (DIC; i.e., mostly bicarbonate (HCO_3^-) and free CO_2 in our case) levels in the water samples. In each of the 13 sampling trips, one 500 ml bottle of water was carefully taken without headspace at each location. After return to the lab, three 100 ml subsamples were taken from each bottle and analyzed immediately. The DIC was then calculated by using the alkalinity titration method (Wetzel & Likens, 2000) (Data S2.4). We found no significant difference of DOC, POC, and DIC among the three inlets and the data were pooled.

Calculation of hydrologic carbon fluxes

Two methods were applied to calculate the annual integrals of lateral DOC, POC, and DIC fluxes (F_{DOC}, F_{POC}, and F_{DIC}). First, we applied Method 5 in Walling & Webb (1985) to calculate the discharge-weighted mean concentrations of DOC, POC, and DIC for each year (Method 1). The annual fluxes were then determined by multiplying the weighted concentrations with the annual integrals of Q_{in} and Q_{out}:

$$F_X = \frac{K\sum_{i=i}^{n}(C_{Xi}Q_i)}{\sum_{i=1}^{n}Q_i}Q_T \quad (5)$$

where F_X and C_{Xi} denote the annual flux and instantaneous concentration (at sampling time (i) of target carbon X (i.e., DOC, POC, DIC), K and n indicate the unit conversion factor and sample number, and Q_i and Q_T indicate the instantaneous discharge at sampling time i, and the annual mean discharge.

Second, we estimated the daily DOC, POC, and DIC (only in 2013) concentrations through the linear interpolation between the sampling trips (Juutinen *et al*., 2013; Wallin *et al*., 2013). The first and last water samples of each year were extrapolated to the start and end of the ice-free period. The interpolated and extrapolated concentrations were then multiplied with the daily Q_{in} and Q_{out} to generate the daily F_{DOC}, F_{POC}, and F_{DIC} at the inlets and outlet (Method 2). Because the water samples were taken at a relatively sparse frequency in comparison with other flux measurements (e.g., F_{CO2}, F_{CH4}), we adopted these two different methods to provide a better constraint in our estimations (Data S2.5). Unless specified, the average of the two estimates was used while reporting the annual hydrologic carbon fluxes. The second method also provided an approximate estimate of seasonality in these hydrologic carbon fluxes.

Sediment core and radioactive dating

The sedimentation rate was determined using the activities of radio-isotope cesium-137 (^{137}Cs) in sediment cores (Bernal & Mitsch, 2012; Mitsch *et al*., 2012). The cores were taken from the deepest water area (~0.6 m at the time of sampling) on 30 October in 2013 (Figure S1). We used gamma ray spectroscopy and followed the same analysis protocol as in our previous studies (Gottgens *et al*., 1999; Spongberg *et al*., 2004) (Data S3). The onset of ^{137}Cs (>0.005 Bq g^{-1}) activities in the sediment profile corresponded to 1966 ± 2 (±SD) based on earlier ^{210}Pb activity dating at the same marsh (Gottgens & Liptak, 1998; Spongberg *et al*., 2004). The long-term (1966–2013) average sediment and organic carbon deposition rates were calculated by dividing the total sediments and organic carbon above the ^{137}Cs onset layer by 48 years. In addition, we compared the total organic carbon above the ^{137}Cs onset layer between our sediment profiles and previous ones taken in 1997 (Muller, 2004). The difference of accumulated organic carbon then provided an estimate of sediment carbon accumulation over the last 16 years (1998–2013).

Statistical Analysis

All of the statistical tests and model fittings were conducted by the R language (R Development Core Team, 2013, version 3.0.0). The parameter estimation in the F_{CO2} partitioning was conducted using the 'nlreg' package (Bellio & Brazzale, 2003). The linear regressions of F_{CH4}, the validation of the simulated and observed Q_{in} and Q_{out}, and the comparisons of the DOC, POC, and DIC among years, seasons, and locations were conducted using the 'lm' function. Unless specified, the significance level was set to 0.05 and the uncertainty (±) always refers to 95% confidence or quantile intervals in the following sections.

Results

Microclimate condition

Our three-year study experienced climate conditions that were extreme outliers over the last 121 years of recorded observations. The year 2012 was the second warmest year (1.9 °C higher than the long-term average of 10.1 °C) of the century in the region (Figure S2a). The 2011–2012 winter (December, 2011 to February, 2012) was exceptionally warm (average: 0.5 °C) in comparison to the long-term average of −2.4 °C. We observed that surface ice melted and reformed during periods with relatively warm temperature (e.g., 17–21 January). The surface ice thawed completely around 13 February, which was much earlier than that in 2011 (26 February) and 2013 (23 February). The warm 2011–2012 winter was followed by an earlier warm-up on 11–25 March. T_a increased drastically to ~20 °C during this early spring period, which was around 15 °C higher than the long-term average. The year of 2011, on the other hand, had the highest amount of annual PP (~1339 mm) over the last

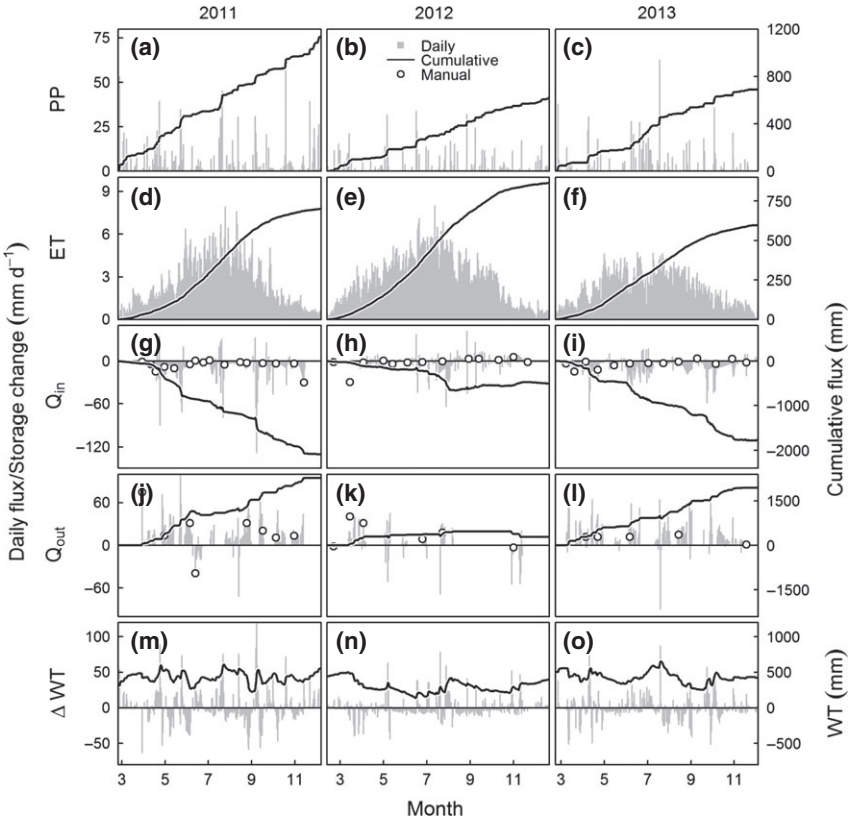

Fig. 1 Time series of the daily water fluxes and storage changes during the ice-free season from 2011 to 2013, including (a–c) precipitation (PP), (d–f) evapotranspiration (ET), (g–i) surface water flow at the inlets (Q_{in}), (j–l) surface water flow at the outlet (Q_{out}), and (m–o) surface water table change (ΔWT). Solid lines indicate the cumulative fluxes (a–l) and storage changes (m–o) starting from the first day of the ice-free season (26 February 2011, 13 February 2012, and 23 February 2013). Q_{in} and Q_{out} are presented in a marsh-area-specific unit. Positive sign convention is adopted for PP. Positive Q_{in}, Q_{out}, and ET indicate the net water flux from the marsh to the nearby ditches or the atmosphere. Positive ΔWT indicates a net increase in the water table (WT) within a daily interval. Open circles (g–l) show the *in situ* manually measured Q_{in} and Q_{out}.

121 years (~490 mm higher than the long-term average) (Fig. 1c).

The climate conditions in 2013 were less extreme in comparison with 2011 and 2012 (Figures S2a, S2c, and 1c). The mean T_a and annual PP were near the long-term averages. However, there were long-lasting rainy periods and cool spells in the summer of 2013. From 22 June to 22 July, the cumulative global radiation (R_g) was 23% and 25% lower in 2013 than 2011 and 2012 (Figure S2c). Following the period with reduced R_g, T_a dropped quickly and reached a local minimum of ~13.2 °C at dawn on 28 July. On average, T_a was ~20.8 °C in the peak summer period (23 July to 22 August) in 2013, which was 2.3–3.5 °C cooler than 2011 and 2012 (Figure S2a). Surface ice started to form around 8 December in 2011, 21 December in 2012, and 5 December in 2013. The cumulative precipitation (mostly as snowfalls) was 206, 134, and 210 mm during the ice-cover periods in 2011, 2012, and 2013, respectively.

Water budget

The three-year water budget showed large interannual variations in both the magnitude of water fluxes and the partitioning among these fluxes (Figs 1a–f and m–o). The extremely wet 2011 had 1133 mm of PP during the ice-free period. ET returned ~700 ± 40 mm (62% of PP) of water back to the atmosphere. The excess water was drained by the Q_{net} (183 ± 67 mm) and also led to a ~250 mm increase in the surface water level. The extremely warm 2012 had the lowest PP in the ice-free period (631 mm) among the 3 years. The ET rate, in contrast, was largely enhanced in the warm and dry year and returned ~865 ± 40 mm (137% of PP) of water back to the atmosphere in the ice-free period. The high ET was largely supplemented by the Q_{net} (−229 ± 51 mm) (i.e., net runoff surplus). The year 2013 had the lowest ice-free-period ET of ~597 ± 40 mm (87% of PP) among the three years.

The partitioned Q_{in} and Q_{out} revealed that the flow regime was characterized by low baseline inflow and intermittently high inflow/outflow (Figs 1g–l). Overall, the majority of Q_{in} values were between 5 and -15 mm day^{-1}. Pulsing inflows occurred only shortly after rainfalls. There were a few peak inflows (-60 to -100 mm day^{-1}) that occurred 1–3 days after intense rainfall events in 2011. Q_{out}, in contrast, occurred only for a relatively shorter period of time (mostly 1–3 days) but had a high volume of water flow. Because of the bimodal pattern in the flow regime, our partitioning approach adequately separated the Q_{net} into Q_{in} and Q_{out} in most of the periods (Data S2 and Figure S3). In sum, 2011 had the highest Q_{in} and Q_{out} of -2087 ± 106 and 2270 ± 146 mm in the ice-free season among the 3 years, while 2012 had the lowest Q_{in} and Q_{out} of -509 ± 73 and 280 ± 95 mm. 2013 had surprisingly high Q_{in} (-1768 ± 99 mm) and Q_{out} (1945 ± 125 mm) after considering that PP was not exceptionally high in the ice-free season. The high Q_{in} in 2013 suggested that there was a large amount of excess water in the upstream croplands, which was partially contributed by snowmelt accumulated in the winter (~177 mm in total). In addition, the decreased ET in the cool summer may have contributed to high surface runoff in the upstream croplands.

Net ecosystem CO_2 exchange

Our three-year study revealed that the annual F_{CO2} was the small residual of two large and opposite fluxes (i.e., GEP and ER). While there was only 5–15% and 5–12% of interannual variation in the annual GEP and ER within the 3 years, these changes in the GEP and ER led to a disproportional and directional change in the annual F_{CO2} (Fig. 2a and Table 1). Surprisingly, the daily F_{CO2} turned positive much earlier in 2013 (~19 August) than 2011 and 2012. The cumulative F_{CO2} was

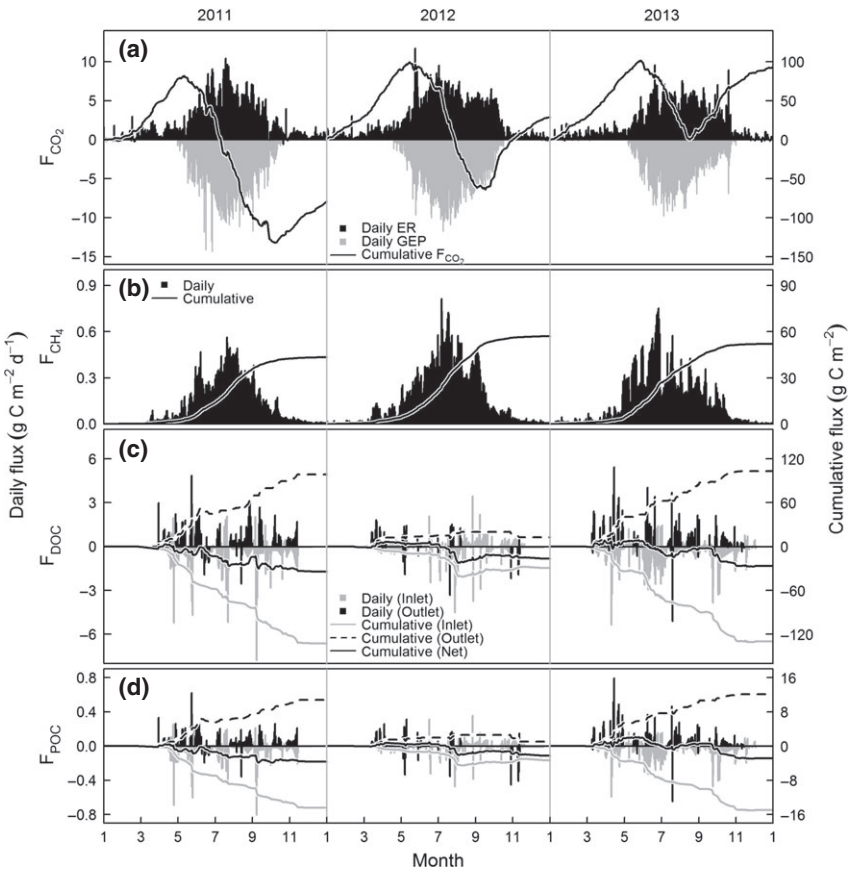

Fig. 2 Time series of the daily carbon fluxes from 2011 to 2013, including the (a) net ecosystem CO_2 exchange (F_{CO2}), (b) net ecosystem CH_4 exchanges (F_{CH4}), (c) dissolved organic carbon flux (F_{DOC}), and (d) particulate organic carbon flux (F_{POC}). The daily F_{CO2} is partitioned and presented as the gross ecosystem production (GEP, grey bars) and ecosystem respiration (ER, black bars). Grey and black bars indicate the fluxes at the inlets and outlet in Figs 2c and 2d. Solid lines indicate the cumulative F_{CO2}, F_{CH4}, F_{DOC}, and F_{POC} starting from 1 January of each year. Grey and dashed lines show the net cumulative fluxes at the inlets and at the outlet in Figs 2c and 2d. Negative sign conventions for all of the fluxes indicate net fluxes into the marsh.

Table 1 Summary of the annual carbon fluxes (g C m^{-2} yr^{-1}) from 2011 to 2013

	2011	2012	2013
Net ecosystem exchange (NEE)			
F_{CO2}	−78.8 ± 33.6	29.7 ± 37.2	92.9 ± 28.0
GEP	−910.8 ± 20.3	−952.4 ± 22.8	−727.4 ± 17.7
ER	832.1 ± 35.3	982.1 ± 40.5	820.4 ± 29.6
F_{CH4}	43.4 ± 1.3	57.0 ± 1.9	52.1 ± 1.8
Hydrologic flux (HF)*			
Inlets			
F_{DOC}	−130.6 ± 10.0	−31.1 ± 11.5	−130.6 ± 13.5
	−132.5 ± 13.8	−29.5 ± 10.3	−130.0 ± 17.5
F_{POC}	−14.5 ± 1.3	−3.2 ± 1.2	−15.0 ± 1.7
	−14.4 ± 1.7	−3.3 ± 1.2	−15.0 ± 2.2
F_{DIC}	n.a.	n.a.	−19.2 ± 2.0
	n.a.	n.a.	−22.1 ± 3.1
Outlet			
F_{DOC}	110.9 ± 10.1	14.4 ± 23.4	125.4 ± 14.0
	98.3 ± 12.7	12.8 ± 7.5	103.3 ± 15.8
F_{POC}	11.4 ± 1.2	0.9 ± 1.2	15.5 ± 2.0
	10.8 ± 1.6	1.0 ± 1.3	12.1 ± 1.9
F_{DIC}	n.a.	n.a.	19.1 ± 2.4
	n.a.	n.a.	18.5 ± 2.4
Carbon balance			
NEE	−35.4 ± 33.7	86.7 ± 37.2	145.0 ± 28.0
HF	−30.3 ± 19.1	−19.0 ± 14.6	−18.9 ± 32.4
NEE + HF	−65.7 ± 38.7	67.7 ± 40.0	126.1 ± 42.8

Negative values indicate net carbon fluxes into the marsh. F_{CO2}, net ecosystem CO_2 exchange; GEP, gross ecosystem production; ER, ecosystem respiration; F_{CH4}, net ecosystem CH_4 exchange; F_{DOC}, dissolved organic carbon flux; F_{POC}, particulate organic carbon flux; F_{DIC}, dissolved inorganic carbon flux; ±, uncertainty intervals; n.a., data not available.

*Annual hydrologic fluxes are calculated using both the Method 1 (line 1) and Method 2 (line 2). Details of the methods are discussed in the Materials and Methods (section 2.4). Annual carbon balances are calculated using the mean hydrological fluxes from the Method 1 and Method 2.

~67.4 g C m^{-2} during the last 67 days of the growing season in 2013, which offset ~73% of the CO_2 uptake in the precedent periods of the growing season.

Our GEP model estimation showed that the interannual variation in GEP was mainly caused by the varied maximal ecosystem CO_2 uptake rates [i.e., P_{max}, Eqn (2)]. The P_{max} (±SD) was 12.8 ± 1.4 μmol CO_2 m^{-2} s^{-1} in the growing season of 2013 (Table S4), which was lower than 20.8 ± 2.7 and 17.2 ± 1.9 μmol CO_2 m^{-2} s^{-1} in 2011 and 2012 ($P = 0.008$ and $P = 0.073$), respectively. In addition, we found that P_{max} declined considerably in the second half of the growing season in 2013, during which P_{max} dropped ~20% to 10.7 ± 0.9 μmol CO_2 m^{-2} s^{-1} after mid-August. Consequently, the reduced P_{max} led to low GEP in 2013, which was ~183–225 g C m^{-2} lower than that in 2011 and 2012.

The base ecosystem respiration [i.e., R_{ref}, Eqn (1)], in contrast, was not different among the 3 years and was relatively constant through the growing seasons (Table S4). R_{ref} ranged around 2.7–2.9 and 0.7–1.5 μmol CO_2 m^{-2} s^{-1} in the growing and nongrowing season, respectively. Because R_{ref} was relatively constant in the growing season, the increasing ER in the late growing season in 2012 resulted mainly from warm temperature anomalies during the period (Fig. 2a and Figure S2a).

Net ecosystem CH_4 exchange

The marsh was an evident and consistent CH_4 source ranging from 43.4 to 57.0 g C m^{-2} yr^{-1} (Fig. 2b and Table 1). The seasonality of F_{CH4} was mainly regulated by the dynamics of T_g (Figure S4, $P < 0.001$, $R^2 = 0.89$), with no significant differences in the temperature sensitivities (0.21 ± 0.01) among these years. On the other hand, we found that the base F_{CH4} at T_g of 14 °C [i.e., R_{FCH4}, Eqn (3)] varied significantly among the 3 years (0.053 and 0.063 g C m^{-2} day^{-1} in 2011 and 2012, respectively). The R_{FCH4} in 2013 was higher than that in 2011 and 2012, with a surprisingly significant decrease in R_{FCH4} after July in 2013 (Figure S4b, $P < 0.001$). R_{FCH4} was 0.088 g C m^{-2} day^{-1} for the period between January and June and decreased to 0.049 g C m^{-2} day^{-1} after that.

Overall, the combination of the interannual variability in both the T_g and R_{FCH4} explained the observed interannual variability in F_{CH4}. 2011 had lower average T_g (13.0 °C) and the lowest R_{FCH4} and consequently the lowest annual F_{CH4} of 43.4 ± 1.3 g C m^{-2} yr^{-1}. In contrast, 2012 had both higher average T_g (14.2 °C) and R_{FCH4} and altogether led to the highest annual F_{CH4} of 57.0 ± 1.9 g C m^{-2} yr^{-1}. 2013 had the lowest annual T_g (12.9 °C) among the 3 years; however, the high R_{FCH4}, especially in the first half of the year, led to an annual F_{CH4} of 52.1 ± 1.8 g C m^{-2} yr^{-1}.

Hydrologic carbon concentrations and fluxes

Dissolved organic carbon was the dominant hydrologic carbon in all sampling locations and trips and was one order of magnitude larger than POC and DIC (Figs 3 and 4a). We found no interannual difference in DOC and POC (Fig. 3). The discharge-weighted DOC concentrations were 62.6 ± 10.0, 61.1 ± 11.5, and 73.8 ± 13.4 mg C l^{-1} in 2011, 2012, and 2013 at the inlets, and 48.9 ± 10.1, 51.3 ± 23.4, and 64.5 ± 13.9 mg C l^{-1} at the outlet (Table S5). We found weak seasonality in DOC and POC that peaked in the early growing season (May–June) in 2011 and

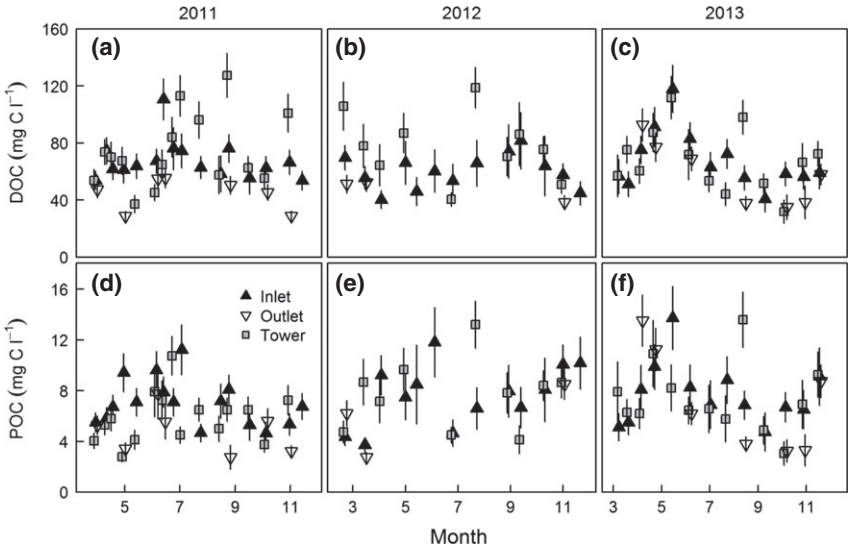

Fig. 3 Time series of the (a–c) dissolved organic carbon (DOC) and (d–f) particulate organic carbon (POC) at the inlets (closed triangles), near the tower (grey squares), and at the outlet (reversed open triangles). Vertical segments indicate the uncertainty intervals incorporating the sample variation and analytical errors.

2013 (DOC and POC: 90–130 and 9–13 mg C l^{-1}). DIC was generally higher in late summer and fall in 2013 (Fig. 4a) in correspondence with the periods that ER exceeded GEP and led to positive F_{CO2} (Fig. 2a). The observed Q_{in} and Q_{out} were not exceptionally high during these high concentration events. No correlation was found between the concentrations and discharges. Thus, linear interpolation among sampling was adopted in generating the daily DOC, POC and DIC (2013). Aside from these few, high concentration data, DOC, POC, and DIC ranged around 40–80, 4–10, and 6–13 mg C l^{-1}, respectively.

Among all of the sampling locations, DOC and POC concentrations were generally lower at the outlet and were compatible at the inlets and near the tower (Fig. 3). Within the 17 trips that water samples were taken at inlets, outlet, and tower, the pairwise comparison showed that DOC and POC were ~38% and ~31% higher at the inlets than that at the outlet ($P < 0.001$ and $P = 0.001$). We adopted the multiplicative relations (i.e., 1.38:1 and 1.31:1) to estimate the outlet DOC and POC for those trips when water samples were only taken at the inlets. The estimated DOC and POC were only used in interpolating the daily DOC and POC for the daily F_{DOC} and F_{POC} calculation. Within the seven sampling trips when DIC was sampled at all locations in 2013, water near the tower had the highest DIC (11.3 mg C l^{-1}, $P = 0.006$) (Fig. 4a), suggesting that high respiration/decomposition occurred within the marsh. On the other hand, we found no significant DIC difference between the inlets (9.8 mg C l^{-1}) and outlet (10.1 mg C l^{-1}).

Our calculated F_{DOC}, F_{POC}, and F_{DIC} showed a pulsing inflow/outflow pattern largely driven by the intermittent Q_{in} and Q_{out} (Figs 2c, d, and 4b). The majority of F_{DOC}, F_{POC}, and F_{DIC} at the inflows were low, with persistent base flows ranged from 0 to −2, from 0 to −0.2, and from 0 to −0.2 g C m^{-2} day^{-1}, respectively. Because Q_{in} and Q_{out} had much greater temporal variations than DOC and POC, the peak F_{DOC}, F_{POC}, and F_{DIC} were dominantly driven by the intermittent peak water flows. The peak F_{DOC}, F_{POC}, and F_{DIC} occurred quickly following intense rainfall events and reached up to −6, −0.6, and −0.6 g C m^{-2} day^{-1}, respectively. These intense but intermittent events significantly influenced the short-term carbon budget. For example, F_{DOC} and F_{POC} increased drastically 1–2 days after the intense rainfalls on 6–8 September in 2011 and peaked on 7 September (Figs 2c and 2d). From 6 to 10 September, the cumulative F_{DOC} and F_{POC} at the inlets were −14.9 and −1.5 g C m^{-2}, respectively. There was no outflow during the period because the outflow gate was closed. The cumulative GEP and ER were −20.0 and 17.4 g C m^{-2} during the same period and led to a slight sink of F_{CO2} (−2.6 ± 1.5 g C m^{-2}). Consequently, F_{DOC} became the largest carbon inflow in this short period. It should also be noted that F_{DOC} and F_{POC} at the inlets turned positive (i.e., reversed flow) in the late summer period in 2012 (Fig. 2c and d). In total, the reversed flows exported ~13.3 and ~1.5 g C m^{-2} of DOC and POC back to the upstream ditches from 9 August to 19 November. As we found that DIC was not significantly different between the inlets

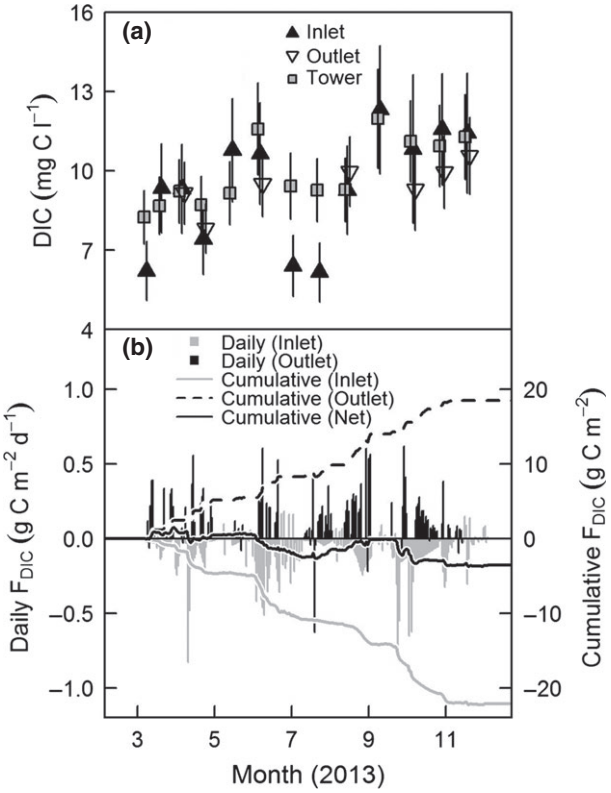

Fig. 4 Time series of the (a) dissolved inorganic carbon concentration (DIC) and (b) daily DIC fluxes (F_{DIC}) in 2013. DIC were measured at the inlets (closed triangles), near the tower (grey squares), and at the outlet (reversed open triangles). Vertical segments in Fig. 4a indicate the uncertainty intervals incorporating the sample variation and analytical errors. Grey and black bars in Fig. 4b indicate the daily F_{DIC} at the inlets and outlet, respectively. Solid, grey, and dashed lines in Fig. 4b indicate the cumulative F_{DIC} starting from 23 February in total, at the inlets, and at the outlet, respectively. Negative F_{DIC} indicates a net flux into the marsh.

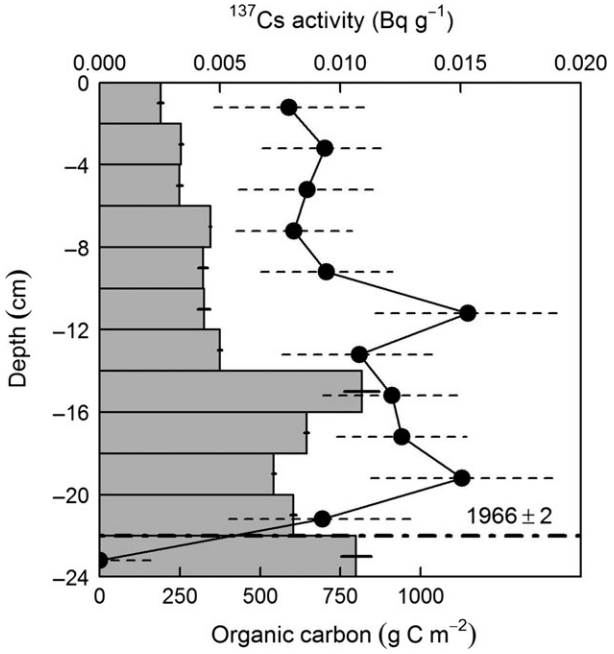

Fig. 5 Profile of the organic carbon content (grey bars) and ^{137}Cs activity (closed circles) for the sediment core. Horizontal solid and dashed segments indicate the uncertainty levels (±SD) of the organic carbon content and ^{137}Cs activity, respectively. The onset of ^{137}Cs activity (~0.005 Bq g^{-1}) corresponds to 1966 ± 2 (±SD) (dash-dotted line).

and outlet, the seasonality of F_{DIC} was largely driven by the dynamics of Q_{in} and Q_{out} (Fig. 4b).

Sediment and organic carbon deposition rate

The marsh sequestered ~4556 ± 29 (±SD) g C m^{-2} of organic carbon in the sediments since ~1966, within which ~33% (~1517 g C m^{-2}) accumulated after 1998. The long-term (1966–2013) average sediment and organic carbon deposition rates were 983.0 ± 84.0 g m^{-2} yr^{-1} and 96.9 ± 10.3 g C m^{-2} yr^{-1} (Fig. 5), respectively. Organic carbon deposition rate in the last 16-year (1998–2013) was ~94.8 g C m^{-2} yr^{-1}, which was compatible with the 48-year average. We found that ^{137}Cs activities increased significantly from 0.000 ± 0.002 (±SD) Bq g^{-1} at the depths of 22–24 cm to 0.009 ± 0.004 Bq g^{-1} at the depths of 20–22 cm. The onset of ^{137}Cs activities occurred at the depth of ~22 cm in the sediments (Fig. 5).

Carbon budget

Both F_{CO2} and F_{CH4} were significant in the atmospheric carbon budget of the marsh (Fig. 6 and Table 1). On an annual basis, GEP and ER largely compensated each other and led to a CO_2 sink in 2011 (−78.8 ± 33.6 g C m^{-2} yr^{-1}), near CO_2 neutral in 2012 (29.7 ± 37.2 g C m^{-2} yr^{-1}), and a CO_2 source in 2013 (92.9 ± 28.0 g C m^{-2} yr^{-1}). On the other hand, F_{CH4} was consistent and evident in all of the study years (43.4–57.0 g C m^{-2} yr^{-1}). The high F_{CH4} offset 55% of the carbon uptake via F_{CO2} in 2011 and led to a slight atmospheric carbon uptake of −35.4 ± 33.7 g C m^{-2} yr^{-1} in 2011. In 2012 and 2013, the sum of ER and F_{CH4} surprisingly exceeded the CO_2 uptake via GEP and both F_{CO2} and F_{CH4} contributed to the atmospheric carbon loss (86.3 ± 37.2 and 145.0 ± 28.0 g C m^{-2} yr^{-1}).

Both F_{POC} and F_{DOC} varied considerably within the 3-year study period (Fig. 6 and Table 1). We found order-of-magnitude interannual differences in the hydrologic carbon fluxes, which were much larger than those in F_{CO2} and F_{CH4}. Overall, F_{DOC} accounted for the

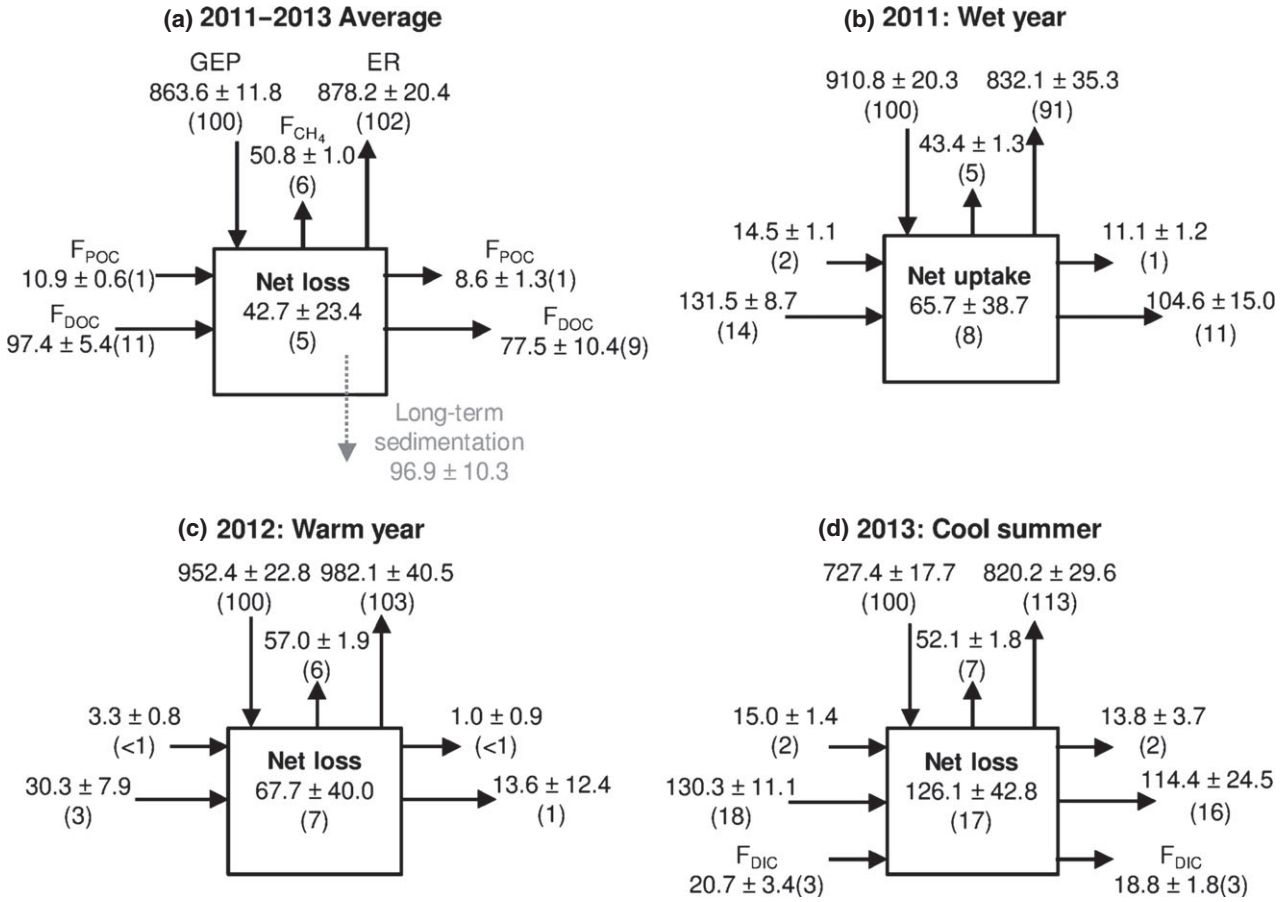

Fig. 6 (a) Three-year average carbon budget and the annual carbon budget in (b) 2011, (c) 2012, and (d) 2013, including the gross ecosystem production (GEP), ecosystem respiration (ER), net ecosystem CH_4 exchanges (F_{CH4}), dissolved organic carbon flux (F_{DOC}), particulate organic carbon flux (F_{POC}), and dissolved inorganic carbon flux (F_{DIC}). The values of net uptake/loss indicated the net ecosystem carbon balance of GEP, ER, F_{CH4}, F_{DOC}, F_{POC}, and F_{DIC} (only in 2013). All fluxes are presented with absolute values (g C m^{-2} yr^{-1}, ±95% uncertainty intervals) while the arrows indicate the flux direction. Values in the parentheses show the relative magnitude (%) of each flux normalized with the GEP in the same year. The grey dashed arrow in Fig. 6a showed the long-term (1966–2013) carbon burial rate in the sediment.

majority of the hydrologic carbon fluxes while F_{POC} and F_{DIC} were equivalent to 8–11% of F_{DOC}. Substantial hydrologic carbon (DOC + POC) fluxes occurred at both the inlets (−146.0 and −145.3 g C m^{-2} yr^{-1}) and the outlet (115.7 and 128.2 g C m^{-2} yr^{-1}) in 2011 and 2013, respectively. On an annual basis, these 2 years had hydrologic carbon inflows equivalent to 16–20% of the carbon uptake via GEP. Yet, 79–88% of the imported carbon was exported to the downstream ditches within the same year. In total, the net hydrologic carbon import was 30.3 ± 19.1 g C m^{-2} in 2011 and became insignificant (18.9 ± 32.4 g C m^{-2}) in 2013. Not surprisingly, F_{DOC} and F_{POC} decreased at both the inlets (−30.3 and −3.3 g C m^{-2} yr^{-1}) and the outlet (13.6 and 1.0 g C m^{-2} yr^{-1}) in the warm and dry year of 2012. The decline of F_{DOC} and F_{POC} was mainly caused by the reduced Q_{in} and Q_{out}. In addition, the reversed Q_{in} in the late summer exported ~14.8 g C m^{-2} back to the upstream ditches and offset ~31% of the DOC and POC imports in the precedent period. Consequently, the net hydrologic carbon import was ~37% lower in 2012 than that in 2011. F_{DIC} at the inlets and the outlet generally compensated each other and, in total, contributed only 1.9 g C m^{-2} to the annual carbon budget in 2013.

The 3-year carbon budget (F_{CO2}, F_{CH4}, F_{DOC}, and F_{POC}) revealed that the marsh was a slight carbon source of 42.7 ± 23.4 g C m^{-2} yr^{-1} (Fig. 6a), which was inconsistent with the long-term carbon accumulation trend in the sediments (96.9 ± 10.3 g C m^{-2} yr^{-1}). On average, the marsh sequestered 863.6 ± 11.8 g C m^{-2} yr^{-1} via GEP. The atmospheric carbon loss from ER and F_{CH4} was equivalent to 102% and 7% of GEP, respectively. The hydrologic carbon (DOC + POC)

inflows and outflows were equivalent to 16% and 12% of GEP, respectively. Within the 3 years, the marsh turned from a carbon sink (-65.7 ± 38.7 g C m^{-2}) in 2011 to a carbon source in 2012 and 2013 (67.7 ± 40.0 and 126.1 ± 42.8 g C m^{-2}) (Figs 6b–d and Table 1). The marsh accumulated ~30.3 ± 19.1 g C m^{-2} via DOC and POC in 2011 and the imported carbon was equivalent to 38% of the net carbon uptake by F_{CO2}. In 2012 and 2013, the hydrologic carbon fluxes compensated 22% and 13% of the total atmospheric carbon loss via both F_{CO2} and F_{CH4}.

Discussion

Carbon budget at freshwater marshes

Our findings highlight the importance of examining wetland carbon budgets in the context of a terrestrial-aquatic continuum. Most importantly, lateral hydrologic carbon fluxes should be carefully addressed in wetlands characterized with a flow-through hydrologic regime (Yan *et al*., 2010; Waletzko & Mitsch, 2013). To date, the importance of lateral hydrologic carbon processes has been addressed mostly in lake studies (Table S6), highlighting that lake carbon balance is largely driven by allochthonous carbon imports via lateral hydrologic fluxes (Dillon & Molot, 1997; Stets *et al*., 2009; Einola *et al*., 2011). Allochthonous carbon imports often resulted in respiration exceeding lake primary production and dissolved CO_2 supersaturation in lake water (Cole *et al*., 1994; Jansson *et al*., 2000; Duarte & Prairie, 2005; Tranvik *et al*., 2009). Thus, most lakes were reported to be net heterotrophic acting as net CO_2 sources to the atmosphere (Duarte & Prairie, 2005; Sobek *et al*., 2005). On the other hand, only a few studies have addressed the full carbon balance of wetlands, with most of them conducted at temperate and boreal peatlands (Table S6). These pioneering studies revealed the significance of hydrologic flows in leaching carbon out from the peat-rich wetlands (e.g., Billett *et al*., 2004; Roulet *et al*., 2007; Nilsson *et al*., 2008; Dinsmore *et al*., 2010; Holden *et al*., 2012; Juutinen *et al*., 2013). To the best of our knowledge, our study is the first full carbon balance for a freshwater marsh, where the vertical gaseous and lateral hydrologic carbon fluxes have been simultaneously measured for multiple years. We argue that hydrologic flows play a different role in carbon cycling at flow-through wetlands (e.g., freshwater marshes, riverine wetlands) than in peatlands. We found a large amount of hydrologic carbon flowing into and out of the marsh. The net carbon contribution of these fluxes was determined by the hydrological conditions and the interplay of different pathways in carbon cycling (i.e., outgas, deposit, transform, or outflow) (Waletzko & Mitsch, 2013).

Our study also highlights the need to carefully express the wetland carbon sequestration rates. Bridgham *et al*. (2006) addressed the importance of distinguishing the allochthonous carbon (i.e., imported from nearby ecosystems) from the autochthonous carbon (i.e., the primary production within the wetlands) while quantifying wetland carbon sequestration rates. The three-year average hydrologic carbon import (~23 ± 13 g C m^{-2} yr^{-1}) was compatible with our earlier estimates (8–69 g C m^{-2} yr^{-1}) from the sedimentation records (Gottgens & Liptak, 1998; Muller, 2004). At a regional scale, the allochthonous carbon represents merely the redistribution of carbon among ecosystems (Mccarty & Ritchie, 2002; Bedard-Haughn *et al*., 2006; Bridgham *et al*., 2006). Reporting solely the sediment deposition rate may lead to overestimation in wetland carbon sequestration, because there is often an unknown portion of the deposited carbon that actually originated from allochthonous sources (Gottgens & Liptak, 1998; Bridgham *et al*., 2006).

Gross ecosysytem production and ER were the two largest fluxes in our three-year carbon budget. However, these two fluxes largely compensated each other and led to a near-neutral CO_2 budget over the 3 years. Our previous study documented that the *Nymphaea*-dominated area contributed a relatively larger portion of our measured turbulent fluxes than the *Typha*-dominated area (Chu *et al*., 2014b). As expected, our net CO_2 uptake rate was lower than that reported from a purely *Typha*-dominated marsh (−251-515 g C m^{-2} yr^{-1}) (Rocha & Goulden, 2008). No report of an annual CO_2 budget obtained via the eddy-covariance method at *Nymphaea*- or *Nuphar*-dominated ecosystems was available. Previous biomass-harvest studies reported that net primary production ranged from 54–279, 37–175, and 507–1565 g C m^{-2} yr^{-1} for *Nymphaea*, *Nuphar*, and *Typha* (Allen & Ocevski, 1981; Hejný *et al*., 1981; Twilley *et al*., 1985; Kok *et al*., 1990; Kunii & Aramaki, 1992; Camargo & Florentino, 2000; Rocha & Goulden, 2009), respectively. These reports often neglected the contribution of heterotrophic respiration and involved uncertainties in quantifying belowground production (Larmola *et al*., 2003). Also, the carbon loss during the nongrowing season (119–145 g C m^{-2} in our case) was often ignored (Aurela *et al*., 2002; Lafleur *et al*., 2003). All these issues made a direct comparison of these reports to our annual F_{CO2} questionable. If we assumed that 40–60% of our growing-season ER originated from heterotrophic respiration, we estimated the net primary production {i.e., $|GEP| - [100\% - (40–60\%)] \times |ER|$} would be around 411–559 g C m^{-2}, still within the reasonable range compared with previous reports. It

should be noted that the climate anomaly especially in 2012 and 2013 also affected GEP and ER and led to a lowered CO_2 uptake rate (to be discussed in the last section). The nearly imbalanced annual CO_2 budget (i.e., $|ER| > |GEP|$) suggested an unmistakable amount of sediment/litter carbon and/or laterally imported carbon that was respired and outgassed as CO_2.

We showed the importance of F_{CH4} in freshwater marsh carbon budgets, where the carbon loss via CH_4 emission may not be compensated by net CO_2 uptake. To date, only a relatively small portion of studies has adequately quantified the annual F_{CH4} at freshwater marshes (Bridgham *et al.*, 2006; Chu *et al.*, 2014b). We concurred that freshwater marshes, characterized by long-lasting inundation and plant-modulated gas flow, deserve more attention due to their efficiency in turning over and releasing newly fixed carbon as CH_4 to the atmosphere (Tornberg *et al.*, 1994; Grosse, 1996; Kim *et al.*, 1999; Chu *et al.*, 2014b). Our results showed that, even at a relatively shorter (multiyear) scale, F_{CH4} may offset a large part of the carbon uptake via F_{CO2} on a carbon balance basis. For a less productive year, both F_{CO2} and F_{CH4} may contribute significantly to atmospheric carbon loss.

Uncertainties and challenges in closing the marsh carbon budgets

Exploration of adequate research infrastructure to continuously measure the hydrologic carbon fluxes is urgently needed to better constrain the uncertainties of hydrologic fluxes. Most published studies estimated discharge via site-specific flow rating curves (i.e., discharge vs. water level) (e.g., Billett *et al.*, 2004; Roulet *et al.*, 2007; Dinsmore *et al.*, 2010), but we found that such an approach failed at our site because of its small hydraulic gradient from the upstream ditches to the marsh and from the marsh to the downstream outlet. Thus, even slight changes in water levels may lead to a varied flow regime. In addition, management of the outflow gate changed the hydraulic gradient, causing water flow reversals during certain dry periods (e.g., late summer in 2012) and making it difficult to apply the rating-curve method at our site. Instead, we found that the water budget approach was generally capable of capturing the major flow events and provided an alternative approach in estimating lateral hydrologic flows. However, caution should be exercised especially in estimating and constraining the uncertainties of water flows. Since all terms in the water budget (e.g., PP, ET, and WT) have quite different sources and magnitudes of uncertainties that, in turn, propagate when solving the water budget, the outcome may include a relatively large uncertainty in the calculated water flows. On average, PP, ET, and WT had uncertainties around ~8–12% in the daily fluxes, which propagated to ~25–27% in the daily Q_{in} and Q_{out}. While integrating to annual sums, the uncertainties averaged out and led to ~2–6% of uncertainties in the annual PP, ET, and WT. These uncertainties propagated to ~20–21% in the annual Q_{in} and Q_{out}. It should be noted that the uncertainty calculation of ET included only the random errors and uncertainties associated with the gap-filling procedures and the sensitivity of friction velocity threshold. The potential systematic uncertainties, such as the lack of energy balance closure, were not included and will be discussed in the following section.

Our energy budgets revealed that the turbulent fluxes, especially energy fluxes, may be underestimated in the study. The magnitude of underestimation, however, was difficult to quantify. To date, only a few studies reported the long-term (annual to interannual) energy budgets in wetlands and small lakes (Goulden *et al.*, 2007; Nordbo *et al.*, 2011; Stoy *et al.*, 2013). As water has a large heat storage capacity, challenges arise when attempting to quantify the heat storage changes of standing water and/or the lateral heat advection carried by water flows in these aquatic ecosystems (Burba *et al.*, 1999b; Lafleur, 2008; Leuning *et al.*, 2012). Spatial heterogeneity of vegetation types, microtopography, and water levels in wetlands may pose additional uncertainties in closing the energy budget because different energy fluxes/storages are often measured with mismatched source areas (Burba *et al.*, 1999a; Shoemaker *et al.*, 2005; Lafleur, 2008). Most importantly, landscape-scale surface heterogeneity, which prevailed at a much larger spatial scale than the typical footprints of tower-based flux measurements, may introduce mesoscale circulations that contribute to the energy balance of local tower sites (Foken, 2008; Foken *et al.*, 2011; Stoy *et al.*, 2013). These mesoscale circulations, however, cannot be observed by single-tower eddy covariance measurements. With our marsh located in a coastal area adjacent to an extensive agricultural landscape and a large lake, sizeable mesoscale circulations are likely to occur and thus contribute to the imbalanced energy budget as observed. We did not correct the turbulent fluxes with the ratios of energy imbalance because, as stated earlier, different mass and energy fluxes may be influenced unequally by the mesoscale circulations and the correction may introduce additional unknown uncertainties (Baldocchi, 2008). Nonetheless, as ET was likely underestimated (not overestimated) in our case, our Q_{in} and thus hydrologic carbon inflow may be treated as a conservative estimate. If we assumed arbitrarily a 10% or 30% underestimation in ET, the hydrologic carbon inflows (DOC + POC) would increase ~5 or ~16 g C m^{-2} yr^{-1}.

More attention is needed to explore and test affordable monitoring systems for *in situ* hydrologic carbon content measurements (e.g., DOC). While we have carefully examined and estimated different sources of uncertainties (e.g., analytical, instrumental, methodological) of hydrologic carbon fluxes, unaccounted (or unknown) uncertainties remained that cannot be assessed based on our current design. This included the temporal dynamics in water carbon contents. Similar to several previous studies (Hope *et al*., 1997; Billett *et al*., 2004; Dawson *et al*., 2004; Holden *et al*., 2012), we found no clear relation between carbon content and discharge. The uncertainties associated with the interpolation of carbon concentrations among sampling trips (i.e., unaccounted temporal variability) were difficult to constrain while calculating the annual integrals of hydrologic carbon fluxes. The two approaches we adopted in integrating annual hydrologic carbon fluxes showed minor deviations in the annual F_{DOC} (0.6–1.9 g C m^{-2} yr^{-1}) and F_{POC} (0.0–0.1 g C m^{-2} yr^{-1}) at the inlets. In contrast, there were 1.6–22.1 (F_{DOC}) and 0.1–3.4 (F_{POC}) g C m^{-2} yr^{-1} differences in annual flux integrals at the outlet. The relatively larger discrepancy in the outlet fluxes revealed the consequence of outflows being sampled less frequently than inflows. To test the sensitivity of DOC/POC interpolation on F_{DOC} and F_{POC} calculations, we used the Monte Carlo simulations (N = 1000) to draw random values of DOC and POC based on the means and standard deviations of our samples (Table S5). The randomly generated DOC and POC values were then adopted to calculate F_{DOC} and F_{POC} for those nonsampling days. We found that most (80–94%) of the simulations generated annual F_{DOC} and F_{POC} that fell within our reported uncertainty levels in F_{DOC} and F_{POC}. A few studies reported random errors associated with sampling frequency as ~5% and ~15% for DOC that was sampled every 20 days (Littlewood, 1995) and every month (Worrall & Burt, 2007), respectively. Considering the sampling-frequency errors, our uncertainty levels of F_{DOC} may increase ~0.3–3.4 g C m^{-2} yr^{-1}. For suspended organic materials (e.g., POC), it was reported that 14- and 21-day sampling intervals may lead to ~18% and ~29% of underestimation (Webb *et al*., 1997). This means that the net POC imports may increase slightly (~0.1–0.6 g C m^{-2} yr^{-1}) compared to our current estimates. Based on these estimates, the sampling frequency should pose minor influence on the interpretation of our marsh carbon budget.

The discrepancy between the three-year carbon budget (F_{CO2}, F_{CH4}, F_{DOC}, and F_{POC}) and the long-term carbon accumulation rate in the sediments revealed the uncertainties and challenges in closing the marsh carbon budget. First, there are knowledge gaps in adequately quantifying the short-term carbon accumulation rates in the sediments (e.g., months to years). The paleoecological approach (i.e., sedimentary isotope profiles) has a temporal resolution of years to decades in these shallow wetlands (Gottgens *et al*., 1999). Multiple-year dynamics (e.g., 2012–2013 in our case) of the carbon balance may not be discriminated by long-term sediment records. Considering the large inherent variability in carbon cycling at wetlands (e.g., Griffis & Rouse, 2001; Lafleur *et al*., 2003; Rocha & Goulden, 2008; Sulman *et al*., 2010), a much longer observation period is required to construct the carbon balance that is comparable with the long-term average sediment burial rate (e.g., ~20 years at a northern peatland; Roulet *et al*., 2007). Imbalanced annual carbon budgets (i.e., exports > imports) were sometimes observed as a consequence of the large interannual variability in F_{CO2} and the depletion of stored carbon (e.g., sediment carbon, standing litter) (Billett *et al*., 2004; Roulet *et al*., 2007; Rocha & Goulden, 2008). The carbon burial rate (96.9 g C m^{-2} yr^{-1}, 1966–2013) was generally compatible with our previous reports (118–156 g C m^{-2} yr^{-1}, 1978–1997) (Gottgens & Liptak, 1998; Spongberg *et al*., 2004). Yet, interpreting carbon burial rates from radioactivity dating at such a short-term and local scale should be done with caution (Clymo *et al*., 1998). ^{137}Cs dating, as widely adopted in quantifying recent (30–50 years) carbon sequestration in wetlands, may overestimate the long-term (century to millennia) average carbon accumulation rates (Craft & Richardson, 1998; Turunen *et al*., 2004). Also, while most studies in freshwater marshes assume a constant sediment/carbon accumulation rate over time (e.g., Reddy *et al*., 1993; Craft & Casey, 2000; Craft, 2007; Bernal & Mitsch, 2012), Clymo *et al.* (1998) argued that the selection of different carbon accumulation models (e.g., linear or quadratic) may have a large effect on the estimation and interpretation of the carbon accumulation rates. In sum, the mismatch of temporal resolution poses difficulties in comparing the multiple-year carbon balance with decadal-to-centurial carbon burial rates (Roulet *et al*., 2007; Juutinen *et al*., 2013).

Second, all of our measured carbon fluxes have different source areas. Our measured gas exchanges (F_{CO2} and F_{CH4}) originated mainly from the 0–250 m fetch near the tower (~15–20 ha), within which floating-leaved vegetation area contributed to the majority of measured turbulent fluxes (Chu *et al*., 2014b). On the other hand, the hydrologic flows have source areas that may extend to the entire marsh basin (~129 ha) consisting of both emergent and floating-leaved vegetation. The source areas for sediment cores are difficult to define and estimate. Sediment cores are usually taken at locations with lower elevation and deeper water. These locations may be subject to sediment focusing.

Thus, our measured sedimentation rates may be higher than the average of the whole marsh (Johnston *et al.*, 2001; Bridgham *et al.*, 2006). In summary, while multiple approaches are needed in quantifying the comprehensive marsh carbon budget, challenges remain in integrating their results into a spatially and temporally comparable framework.

Third, some carbon fluxes and/or storage changes were unaccounted and not quantified in our budgets. Change in carbon storages (e.g., sediment, belowground biomass, standing litter (e.g., *Typha*), and carbon within the water column) may explain a considerable portion of the carbon imbalance in our three-year study. We estimated that ~23 kg C m^{-2} was stored in the sediments, belowground biomass, and water column at the marsh. A slight change in the carbon pool (e.g., 0.1%) would produce a significant change (e.g., ~23 g C m^{-2}) in the carbon budget. Moreover, hydrologic carbon fluxes during the winter may occur when the surface water was not completely frozen. On the basis of the difference in surface water levels between the start and the end of the ice-covered season (only available for December 2011–Febuarary 2012 and December 2012–Febuarary 2013), we estimated that the marsh received ~100–150 mm of water inflow throughout the winter. Adopting the mean hydrologic carbon concentrations from the last sampling trip before and the first sampling trip after the ice-cover periods, the unaccounted winter inflows may import ~10 g C m^{-2} (DOC + POC) to the marsh. Additional DOC and DIC imports via wet deposition were believed to be negligible, with reported values of 0.84–3.21 and 0.15 g C m^{-2} yr^{-1} (Dillon & Molot, 1997; Sobek *et al.*, 2006; Stets *et al.*, 2009), respectively.

Implications of hydrologic carbon fluxes

The importance of hydrologic carbon fluxes should also be viewed in the context of a terrestrial-aquatic landscape. We showed that a significant amount of carbon [43–189 Mg C yr^{-1} (DOC + POC)] was transported from agricultural runoff into the marsh. On average, the carbon inflow was equivalent to a net loss of ~53 g C m^{-2} yr^{-1} from the upstream watershed, which was equivalent to ~35% and ~33% of the annual CO_2 uptake at conventional soybean and corn croplands in productive years (Zenone *et al.*, 2013; Chu *et al.*, 2014b). Despite the large variability among years and crop types, our reported hydrologic carbon inflows suggested an evident and unaccounted amount of carbon that is eroded from the croplands and flows into the downstream wetlands.

We measured 19–165 Mg C yr^{-1} (DOC + POC) flowing out of the marsh into Lake Erie. On average, the carbon outflow was equivalent to a watershed-area-specific carbon export rate of ~29 g C m^{-2} yr^{-1}. To the best of our knowledge, the hydrologic carbon imports through river transport have not been well quantified in the Lake Erie basin. Based on the empirical equation in Schlesinger & Melack (1981), the annual carbon export from the nearby Sandusky River was estimated to be ~15 Pg C yr^{-1}, which was equivalent to a watershed area specific carbon export rate of ~4 g C m^{-2} yr^{-1}. Bouchard (2007) addressed the implications of carbon outflows from wetlands for supplementing the carbon cycling in Lake Erie. These results were consistent with recent syntheses, such as Tranvik *et al.* (2009), which demonstrated that inland lakes and reservoirs may serve as important regulators in regional and global carbon cycling through large amounts of CO_2/CH_4 emission and sediment deposition. To date, carbon cycling and the full carbon budgets in large lakes (e.g., Lake Erie) are still understudied (Bennington *et al.*, 2012). Further research, especially on CO_2/CH_4 outgassing and river carbon transport, is needed to quantify a comprehensive regional carbon budget.

Responses to climate variability and anomaly

Different carbon fluxes respond unequally to climate anomalies and interannual climatic variability and consequently, the marsh carbon budget may vary greatly among years. Further research should pay attention to the interplay of different carbon processes at wetlands in response to climate extremes. Despite the uncertainties in future greenhouse gas emission trajectories and climate change projection models, most projections show that annual and seasonal temperatures in the Great Lake region could increase significantly in the 21st century (e.g., Wuebbles & Hayhoe, 2004; Hayhoe *et al.*, 2010; Winkler *et al.*, 2012). Wuebbles & Hayhoe (2004) projected that the annual average daily maximum temperature could increase 3–6 °C relative to the 1961–1990 average by the end of the 21st century. They reported that the temperature increase would be especially severe in summer (3–8 °C). We found that annual ER and F_{CH4} were 18% and 31% higher in the extremely warm 2012 than in 2011. While the higher ER can be mostly attributed to higher air temperature, the higher F_{CH4} resulted from both the higher soil temperature and higher R_{FCH4} (i.e., base F_{CH4}). Gross ecosystem production, on the other hand, increased only slightly (~5%) in the warm 2012. Consequently, F_{CO2} and F_{CH4} combined released ~122 g C m^{-2} more carbon to the atmosphere in 2012 than in 2011. This suggests that warmer climate influences the marsh carbon cycling and budget mainly through enhancing ER and F_{CH4}. The underlying mechanisms that govern the in-

terannual variability of base F_{CH4} need more attention. Substrate quality associated with primary production most likely explains the interannual variability of R_{FCH4} (Herbst *et al*., 2011; Chu *et al*., 2014b). Further research, such as manipulated microcosm experiments, should examine how sensitive the base F_{CH4} is to warmer climate conditions.

To our surprise, the cool anomaly in the 2013 summer had a great impact on the marsh carbon cycling and turned the marsh into a significant CO_2 source. More attention should be devoted to evaluate the extent of the impact of such chilling events during the growing season. We found that the summer cool spells influenced the marsh carbon cycling mainly through reducing the maximal CO_2 uptake rate (i.e., P_{max}) and thus GEP. In sum, the annual GEP in 2013 was 20–24% lower than that in 2011–2012. ER, on the other hand, decreased relatively slightly (1–16%) and, consequently, the marsh became a significant CO_2 source (92.9 g C m^{-2} yr^{-1}) in 2013. Again, the disproportional responses of ER and GEP to temperature anomalies deserve more attention because even a small change in these two large carbon fluxes may translate to considerable changes in magnitude and direction of F_{CO2}. Interestingly, we also found that the base F_{CH4} (i.e., R_{FCH4}) decreased significantly after the summer cool spells. The near simultaneous decrease in P_{max} and R_{FCH4} supported our earlier proposition that GEP and F_{CH4} were highly linked in these long-lasting inundated freshwater marshes (Chu *et al*., 2014b). Most importantly, both GEP and F_{CH4} were sensitive to the cool anomaly and responded greatly to the chilling events in the growing season.

Overall, the interannual variability in PP had a significant influence on the lateral hydrologic carbon fluxes and thus the carbon budgets. Compared with temperature, there is even larger uncertainty and discrepancy in projecting PP in the coming decades (Wuebbles & Hayhoe, 2004; Hayhoe *et al*., 2010; Winkler *et al*., 2012). While models remain inconsistent about the projected PP in summer and fall, the winter and spring PP is likely to increase by as much as 20–30% in the Great Lake region in the 21st century (Wuebbles & Hayhoe, 2004; Hayhoe *et al*., 2010). The contrasting PP in 2011 and 2012 (~574 mm difference) provided a valuable opportunity to examine the response of the marsh carbon cycling and budget. We found an order-of-magnitude difference in both the hydrologic carbon inflows and outflows between the wet and dry years. Such a drastic effect of interannual/seasonal variability in precipitation on carbon budgets was also reported in previous studies, where the systems were characterized by a flow-through hydrologic regime (e.g., Einola *et al*., 2011; Ojala *et al*., 2011; Waletzko & Mitsch, 2013). The net carbon contribution of these hydrologic fluxes was then determined as the residual of the two large and opposite fluxes (inflow and outflow).

The strong linkage between the functions of wetlands as carbon sinks or sources and climate, upstream runoff, and downstream outflow suggests large variability in the carbon budgets of freshwater marshes. Both human activities, such as land use change upstream and wetland flow regulations, and climate change in the region are likely to alter the carbon cycling and thus the carbon budgets of the remaining wetlands.

Acknowledgements

This project was funded by the National Oceanic and Atmospheric Administration (NOAA) (NA10OAR4170224) and the National Science Foundation (NSF) (NSF1034791) Field Station and Marine Labs (FSML) program, USA. ARD was supported by NSF (NSF0845166). We thank John Simpson and the Winous Point Marsh Conservancy for fully supporting the research platform and logistical assistance at the Winous Point North Marsh. We thank Richard Becker, Timothy Fisher, James Martin-Hayden, Donald Cahoon, Karen Roderick-Lingema, Asko Noormets, Thomas Bridgeman, Kristin Kirschbaum, Ranjeet John, Barry Muller, Jeremy Pritt, Walter Berger, and Haiqiang Guo for their helpful assistance and advice. We thank the Subject Editor and three anonymous reviewers for providing valuable suggestions for the quality of the study. We gratefully acknowledge Mike Deal, Jianye Xu, Orrin Babcock, Cory Becher, Yahn-Jauh Su, Jing Xie, Terenzio Zenone, and Jennifer Teeple for building and maintaining the site infrastructure and assisting in the data collection and management. We also thank Lisa Delp Taylor for editing the manuscript.

References

Algesten G, Sobek S, Bergström A-K, Ågren A, Tranvik LJ, Jansson M (2004) Role of lakes for organic carbon cycling in the boreal zone. *Global Change Biology*, **10**, 141–147.

Allen HL, Ocevski BT (1981) Comparative primary productivity of algal epiphytes on three species of macrophyte in the littoral zone of Lake Ohrid, Yugoslavia. *Ecography*, **4**, 155–160.

Aufdenkampe AK, Mayorga E, Raymond PA *et al*. (2011) Riverine coupling of biogeochemical cycles between land, oceans, and atmosphere. *Frontiers in Ecology and the Environment*, **9**, 53–60.

Aurela M, Laurila T, Tuovinen J-P (2002) Annual CO_2 balance of a subarctic fen in northern Europe: importance of the wintertime efflux. *Journal of Geophysical Research*, **107**, 4607.

Baldocchi D (2008) Turner review No. 15'.Breathing' of the terrestrial biosphere: lessons learned from a global network of carbon dioxide flux measurement systems. *Australian Journal of Botany*, **56**, 1–26.

Bedard-Haughn A, Jongbloed F, Akkerman J, Uijl A, De Jong E, Yates T, Pennock D (2006) The effects of erosional and management history on soil organic carbon stores in ephemeral wetlands of hummocky agricultural landscapes. *Geoderma*, **135**, 296–306.

Bellio R, Brazzale AR (2003) Higher order asymptotics unleashed: software design for nonlinear heteroscedastic regression. *Journal of Computational and Graphical Statistics*, **12**, 682–697.

Bennington V, Mckinley GA, Urban NR, Mcdonald CP (2012) Can spatial heterogeneity explain the perceived imbalance in Lake Superior's carbon budget? A model study. *Journal of Geophysical Research: Biogeosciences*, **117**, G03020.

Bernal B, Mitsch WJ (2012) Comparing carbon sequestration in temperate freshwater wetland communities. *Global Change Biology*, **18**, 1636–1647.

Billett MF, Palmer SM, Hope D *et al*. (2004) Linking land-atmosphere-stream carbon fluxes in a lowland peatland system. *Global Biogeochemical Cycles*, **18**, GB1024.

Bouchard V (2007) Export of organic matter from a coastal freshwater wetland to Lake Erie: an extension of the outwelling hypothesis. *Aquatic Ecology*, **41**, 1–7.

Bridgham S, Megonigal J, Keller J, Bliss N, Trettin C (2006) The carbon balance of North American wetlands. *Wetlands*, **26**, 889–916.

Buffam I, Turner MG, Desai AR *et al.* (2011) Integrating aquatic and terrestrial components to construct a complete carbon budget for a north temperate lake district. *Global Change Biology*, **17**, 1193–1211.

Burba G, Verma S, Kim J (1999a) A comparative study of surface energy fluxes of three communities (*Phragmites australis*, *Scirpus acutus*, and open water) in a prairie wetland ecosystem. *Wetlands*, **19**, 451–457.

Burba GG, Verma SB, Kim J (1999b) Surface energy fluxes of *Phragmites australis* in a prairie wetland. *Agricultural and Forest Meteorology*, **94**, 31–51.

Camargo A, Florentino E (2000) Population dynamics and net primary production of the aquatic macrophite *Nymphaea rudgeana* CF Mey in a lotic environment of the Itanhaém River basin (SP, Brazil). *Revista Brasileira de Biologia*, **60**, 83–92.

Chu H-S, Chang S-C, Klemm O *et al.* (2014a) Does canopy wetness matter? Evapotranspiration from a subtropical montane cloud forest in Taiwan. *Hydrological Processes*, **28**, 1190–1214.

Chu H, Chen J, Gottgens JF, Ouyang Z, John R, Czajkowski K, Becker R (2014b) Net ecosystem methane and carbon dioxide exchanges in a Lake Erie coastal marsh and a nearby cropland. *Journal of Geophysical Research: Biogeosciences*, **119**, 722–740.

Clymo R, Turunen J, Tolonen K (1998) Carbon accumulation in peatland. *Oikos*, **81**, 368–388.

Cole J, Caraco N, Kling G, Kratz T (1994) Carbon dioxide supersaturation in the surface waters of lakes. *Science*, **265**, 1568–1570.

Cole J, Prairie Y, Caraco N *et al.* (2007) Plumbing the global carbon cycle: Integrating inland waters into the terrestrial carbon budget. *Ecosystems*, **10**, 172–185.

Craft C (2007) Freshwater input structures soil properties, vertical accretion, and nutrient accumulation of Georgia and US tidal marshes. *Limnology and Oceanography*, **52**, 1220–1230.

Craft CB, Casey WP (2000) Sediment and nutrient accumulation in floodplain and depressional freshwater wetlands of Georgia, USA. *Wetlands*, **20**, 323–332.

Craft C, Richardson C (1998) Recent and long-term organic soil accretion and nutrient accumulation in the Everglades. *Soil Science Society of America Journal*, **62**, 834–843.

Dawson JJ, Billett MF, Hope D, Palmer SM, Deacon CM (2004) Sources and sinks of aquatic carbon in a peatland stream continuum. *Biogeochemistry*, **70**, 71–92.

Dean WE (1974) Determination of carbonate and organic matter in calcareous sediments and sedimentary rocks by loss on Ignition: comparison with other methods. *Journal of Sedimentary Research*, **44**, 242–248.

Desai AR, Richardson AD, Moffat AM *et al.* (2008) Cross-site evaluation of eddy covariance GPP and RE decomposition techniques. *Agricultural and Forest Meteorology*, **148**, 821–838.

Dillon PJ, Molot LA (1997) Dissolved organic and inorganic carbon mass balances in central Ontario Lakes. *Biogeochemistry*, **36**, 29–42.

Dinsmore KJ, Billett MF, Skiba UM, Rees RM, Drewer J, Helfter C (2010) Role of the aquatic pathway in the carbon and greenhouse gas budgets of a peatland catchment. *Global Change Biology*, **16**, 2750–2762.

Duarte CM, Prairie YT (2005) Prevalence of heterotrophy and atmospheric CO_2 emissions from aquatic ecosystems. *Ecosystems*, **8**, 862–870.

Einola E, Rantakari M, Kankaala P *et al.* (2011) Carbon pools and fluxes in a chain of five boreal lakes: a dry and wet year comparison. *Journal of Geophysical Research: Biogeosciences*, **116**, G03009.

Falge E, Baldocchi D, Olson R *et al.* (2001) Gap filling strategies for defensible annual sums of net ecosystem exchange. *Agricultural and Forest Meteorology*, **107**, 43–69.

Foken T (2008) The energy balance closure problem: an overview. *Ecological Applications*, **18**, 1351–1367.

Foken T, Aubinet M, Finnigan JJ, Leclerc MY, Mauder M, Paw U KT (2011) Results of a panel discussion about the energy balance closure correction for trace gases. *Bulletin of the American Meteorological Society*, **92**, ES13–ES18.

Gottgens JF, Liptak MA (1998) Longterm assimilation of agricultural runoff in a Lake Erie marsh. *Verhandlungen des Internationalen Verein Limnologie*, **26**, 1337–1342.

Gottgens JF, Rood BE, Delfino JJ, Simmers BS (1999) Uncertainty in paleoecological studies of mercury in sediment cores. *Water, Air, and Soil Pollution*, **110**, 313–333.

Goulden ML, Litvak M, Miller SD (2007) Factors that control *Typha* marsh evapotranspiration. *Aquatic Botany*, **86**, 97–106.

Griffis TJ, Rouse WR (2001) Modelling the interannual variability of net ecosystem CO_2 exchange at a subarctic sedge fen. *Global Change Biology*, **7**, 511–530.

Grosse W (1996) Pressurised ventilation in floating-leaved aquatic macrophytes. *Aquatic Botany*, **54**, 137–150.

Hayhoe K, Vandorn J, Croley Ii T, Schlegal N, Wuebbles D (2010) Regional climate change projections for Chicago and the US Great Lakes. *Journal of Great Lakes Research*, **36**, 7–21.

Heiri O, Lotter AF, Lemcke G (2001) Loss on ignition as a method for estimating organic and carbonate content in sediments: reproducibility and comparability of results. *Journal of Paleolimnology*, **25**, 101–110.

Hejný S, Kvêt J, Dykyjová D (1981) Survey of biomass and net production of higher plant communities in fishponds. *Folia Geobotanica et Phytotaxonomica*, **16**, 73–94.

Herbst M, Friborg T, Ringgaard R, Soegaard H (2011) Interpreting the variations in atmospheric methane fluxes observed above a restored wetland. *Agricultural and Forest Meteorology*, **151**, 841–853.

Holden J, Smart RP, Dinsmore KJ, Baird AJ, Billett MF, Chapman PJ (2012) Natural pipes in blanket peatlands: major point sources for the release of carbon to the aquatic system. *Global Change Biology*, **18**, 3568–3580.

Hope D, Billett MF, Milne R, Brown TA (1997) Exports of organic carbon in British rivers. *Hydrological Processes*, **11**, 325–344.

Jansson M, Bergström A-K, Blomqvist P, Drakare S (2000) Allochthonous organic carbon and phytoplankton/bacterioplankton production relationships in lakes. *Ecology*, **81**, 3250–3255.

Jenerette GD, Lal R (2005) Hydrologic sources of carbon cycling uncertainty throughout the terrestrial-aquatic continuum. *Global Change Biology*, **11**, 1873–1882.

Johnson MS, Lehmann J, Riha SJ, Krusche AV, Richey JE, Ometto JPHB, Couto EG (2008) CO_2 efflux from Amazonian headwater streams represents a significant fate for deep soil respiration. *Geophysical Research Letters*, **35**, L17401.

Johnston CA, Bridgham SD, Schubauer-Berigan JP (2001) Nutrient dynamics in relation to geomorphology of riverine wetlands. *Soil Science Society of America Journal*, **65**, 557–577.

Juutinen S, Väliranta M, Kuutti V *et al.* (2013) Short-term and long-term carbon dynamics in a northern peatland-stream-lake continuum – a catchment approach. *Journal of Geophysical Research: Biogeosciences*, **118**, 1–13.

Kim J, Verma SB, Billesbach DP (1999) Seasonal variation in methane emission from a temperate *Phragmites*-dominated marsh: effect of growth stage and plant-mediated transport. *Global Change Biology*, **5**, 433–440.

Kling GW, Kipphut GW, Miller MC (1991) Arctic lakes and streams as gas conduits to the atmosphere: implications for tundra carbon budgets. *Science*, **251**, 298–301.

Knoll LB, Vanni MJ, Renwick WH, Dittman EK, Gephart JA (2013) Temperate reservoirs are large carbon sinks and small CO_2 sources: results from high-resolution carbon budgets. *Global Biogeochemical Cycles*, **27**, 52–64.

Kok CJ, Van Der Velde G, Landsbergen KM (1990) Production, nutrient dynamics and initial decomposition of floating leaves of *Nymphaea alba* L. and *Nuphar lutea* (L.) Sm. (*Nymphaeaceae*) in alkaline and acid waters. *Biogeochemistry*, **11**, 235–250.

Kormann R, Meixner F (2001) An analytical footprint model for non-neutral stratification. *Boundary-Layer Meteorology*, **99**, 207–224.

Kunii H, Aramaki M (1992) Annual net production and life span of floating leaves in *Nymphaea tetragona* Georgi: a comparison with other floating-leaved macrophytes. *Hydrobiologia*, **242**, 185–193.

Lafleur PM (2008) Connecting atmosphere and wetland: energy and water vapour exchange. *Geography Compass*, **2**, 1027–1057.

Lafleur PM, Roulet NT, Bubier JL, Frolking S, Moore TR (2003) Interannual variability in the peatland-atmosphere carbon dioxide exchange at an ombrotrophic bog. *Global Biogeochemical Cycles*, **17**, 1036.

Larmola T, Alm J, Juutinen S, Martikainen PJ, Silvola J (2003) Ecosystem CO_2 exchange and plant biomass in the littoral zone of a boreal eutrophic lake. *Freshwater Biology*, **48**, 1295–1310.

Leuning R, Van Gorsel E, Massman WJ, Isaac PR (2012) Reflections on the surface energy imbalance problem. *Agricultural and Forest Meteorology*, **156**, 65–74.

Littlewood IG (1995) Hydrological regimes, sampling strategies, and assessment of errors in mass load estimates for United Kingdom rivers. *Environment International*, **21**, 211–220.

Lloyd J, Taylor JA (1994) On the temperature dependence of soil respiration. *Functional Ecology*, **8**, 315–323.

Mahrt L (1998) Flux sampling errors for aircraft and towers. *Journal of Atmospheric and Oceanic Technology*, **15**, 416–429.

Mccarty GW, Ritchie JC (2002) Impact of soil movement on carbon sequestration in agricultural ecosystems. *Environmental Pollution*, **116**, 423–430.

Mitsch WJ, Bernal B, Nahlik AM *et al.* (2012) Wetlands, carbon, and climate change. *Landscape Ecology*, **28**, 583–597.

Muller BE (2004) The effect of long-term nonpoint-source agricultural runoff on assimilative capacity of freshwater marshes: a paleoecological approach. PhD Dissertation, University of Toledo, Toledo, USA.

Nilsson M, Sagerfors J, Buffam I *et al.* (2008) Contemporary carbon accumulation in a boreal oligotrophic minerogenic mire–A significant sink after accounting for all C-fluxes. *Global Change Biology*, **14**, 2317–2332.

Nordbo A, Launiainen S, Mammarella I, Leppäranta M, Huotari J, Ojala A, Vesala T (2011) Long-term energy flux measurements and energy balance over a small boreal lake using eddy covariance technique. *Journal of Geophysical Research: Atmospheres*, **116**, D02119.

Ojala A, Bellido JL, Tulonen T, Kankaala P, Huotari J (2011) Carbon gas fluxes from a brown-water and a clear-water lake in the boreal zone during a summer with extreme rain events. *Limnology and Oceanography*, **56**, 61–76.

Reddy K, Debusk W, Delaune R, Koch M (1993) Long-term nutrient accumulation rates in the Everglades. *Soil Science Society of America Journal*, **57**, 1147–1155.

Reichstein M, Falge E, Baldocchi D *et al.* (2005) On the separation of net ecosystem exchange into assimilation and ecosystem respiration: review and improved algorithm. *Global Change Biology*, **11**, 1424–1439.

Richardson AD, Hollinger DY (2005) Statistical modeling of ecosystem respiration using eddy covariance data: maximum likelihood parameter estimation, and Monte Carlo simulation of model and parameter uncertainty, applied to three simple models. *Agricultural and Forest Meteorology*, **131**, 191–208.

Richardson AD, Hollinger DY, Burba GG *et al.* (2006) A multi-site analysis of random error in tower-based measurements of carbon and energy fluxes. *Agricultural and Forest Meteorology*, **136**, 1–18.

Rocha AV, Goulden ML (2008) Large interannual CO_2 and energy exchange variability in a freshwater marsh under consistent environmental conditions. *Journal of Geophysical Research*, **113**, G04019.

Rocha AV, Goulden ML (2009) Why is marsh productivity so high? New insights from eddy covariance and biomass measurements in a Typha marsh. *Agricultural and Forest Meteorology*, **149**, 159–168.

Roulet NT, Lafleur PM, Richard PJ, Moore TR, Humphreys ER, Bubier J (2007) Contemporary carbon balance and late Holocene carbon accumulation in a northern peatland. *Global Change Biology*, **13**, 397–411.

Schlesinger WH, Melack JM (1981) Transport of organic carbon in the world's rivers. *Tellus*, **33**, 172–187.

Shoemaker WB, Sumner DM, Castillo A (2005) Estimating changes in heat energy stored within a column of wetland surface water and factors controlling their importance in the surface energy budget. *Water Resources Research*, **41**, W10411.

Sobek S, Tranvik LJ, Cole JJ (2005) Temperature independence of carbon dioxide supersaturation in global lakes. *Global Biogeochemical Cycles*, **19**, GB2003.

Sobek S, Söderbäck B, Karlsson S, Andersson E, Brunberg AK (2006) A carbon budget of a small humic lake: an example of the importance of lakes for organic matter cycling in boreal catchments. *AMBIO: A Journal of the Human Environment*, **35**, 469–475.

Spongberg A, Gottgens J, Muller B (2004) Pesticide accumulation rates in a managed marsh along Lake Erie. *Water, Air, and Soil Pollution*, **152**, 387–404.

Stets EG, Striegl RG, Aiken GR, Rosenberry DO, Winter TC (2009) Hydrologic support of carbon dioxide flux revealed by whole–lake carbon budgets. *Journal of Geophysical Research: Biogeosciences*, **114**, G01008.

Stoy PC, Mauder M, Foken T *et al.* (2013) A data-driven analysis of energy balance closure across FLUXNET research sites: the role of landscape scale heterogeneity. *Agricultural and Forest Meteorology*, **171–172**, 137–152.

Sulman BN, Desai AR, Saliendra NZ *et al.* (2010) CO_2 fluxes at northern fens and bogs have opposite responses to inter-annual fluctuations in water table. *Geophysical Research Letters*, **37**, L19702.

Tornberg T, Bendix M, Brix H (1994) Internal gas transport in *Typha latifolia* L. and *Typha angustifolia* L. 2. Convective throughflow pathways and ecological significance. *Aquatic Botany*, **49**, 91–105.

Tranvik LJ, Downing JA, Cotner JB *et al.* (2009) Lakes and reservoirs as regulators of carbon cycling and climate. *Limnology and Oceanography*, **54**, 2298–2314.

Turunen J, Roulet NT, Moore TR, Richard PJ (2004) Nitrogen deposition and increased carbon accumulation in ombrotrophic peatlands in eastern Canada. *Global Biogeochemical Cycles*, **18**, GB3002.

Twilley RR, Blanton LR, Brinson MM, Davis GJ (1985) Biomass production and nutrient cycling in aquatic macrophyte communities of the Chowan River, North Carolina. *Aquatic Botany*, **22**, 231–252.

Waletzko E, Mitsch W (2013) The carbon balance of two riverine wetlands fifteen years after their creation. *Wetlands*, **33**, 989–999.

Wallin MB, Grabs T, Buffam I, Laudon H, Ågren A, Öquist MG, Bishop K (2013) Evasion of CO_2 from streams – The dominant component of the carbon export through the aquatic conduit in a boreal landscape. *Global Change Biology*, **19**, 785–797.

Walling D, Webb B (1985) Estimating the discharge of contaminants to coastal waters by rivers: some cautionary comments. *Marine Pollution Bulletin*, **16**, 488–492.

Webb B, Phillips J, Walling D, Littlewood I, Watts C, Leeks G (1997) Load estimation methodologies for British rivers and their relevance to the LOIS RACS (R) programme. *Science of The Total Environment*, **194–195**, 379–389.

Wetzel RG, Likens GE (2000) *Limnological Analyses*. Springer, New York.

Wilson K, Goldstein A, Falge E *et al.* (2002) Energy balance closure at FLUXNET sites. *Agricultural and Forest Meteorology*, **113**, 223–243.

Winkler JA, Arritt RW, Pryor SC (2012) Climate projections for the midwest: availability, interpretation and synthesis. In:*US National Climate Assessment Midwest Technical Input Report* (eds Winkler J, Andresen J, Hatfield J, Bidwell D, Brown D) pp 1–24. Great Lakes Integrated Sciences and Assessment (GLISA) Center, Ann Arbor, USA.

Worrall F, Burt T (2007) Flux of dissolved organic carbon from UK rivers. *Global Biogeochemical Cycles*, **21**, GB1013.

Wuebbles DJ, Hayhoe K (2004) Climate change projections for the United States Midwest. *Mitigation and Adaptation Strategies for Global Change*, **9**, 335–363.

Yan Y, Guo H, Gao Y, Zhao B, Chen J, Li B, Chen J (2010) Variations of net ecosystem CO_2 exchange in a tidal inundated wetland: coupling MODIS and tower- based fluxes. *Journal of Geophysical Research: Atmosphere*, **115**, D15102.

Zenone T, Gelfand I, Chen J, Hamilton SK, Robertson GP (2013) From set-aside grassland to annual and perennial cellulosic biofuel crops: effects of land use change on carbon balance. *Agricultural and Forest Meteorology*, **182–183**, 1–12.

Supporting Information

Additional Supporting Information may be found in the online version of this article:

Data S1. F_{CO2} Partitioning and Flux Uncertainty Analysis.
Data S2. Hydrologic Carbon Flux Calculation and Uncertainty Analysis.
Data S3. Sediment and Organic Carbon Deposition Rate Analysis.
Figure S1. Map of the Winous Point North Marsh in northwestern Ohio, USA.
Figure S2. Time series of the daily micrometeorological variables.
Figure S3. Comparison of the observed and simulated surface water flow at the inlets (Q_{in}) and outlet (Q_{out}).
Figure S4. Regression models of the daily CH_4 flux against soil temperature.
Table S1. List of micrometeorological sensors at the marsh tower.
Table S2. Summary of gaps in F_{CO2}, F_{CH4}, and ET.
Table S3. Summary of the annual energy budget.
Table S4. Summary of the model coefficients for gross ecosystem production (GEP) and ecosystem respiration (ER).
Table S5. Summary of the discharge-weighted carbon concentrations.
Table S6. Reported annual carbon budgets in freshwater wetlands and small lakes.